

Space Generation Cosmology

A Minimal Parametric Cosmological Model Explaining SN1a and
BAO without Dark Components

[Kwon Minyoung]

May 31, 2025

Contents

1	Introduction	4
2	Model Description	5
2.1	Derivation of Power-Law Expansion $H(z) = H_0(1+z)^n$	5
2.2	Type Ia Supernovae	6
2.2.1	Comparison of Supernova Distance Modulus	7
2.2.2	Comparison of Residuals and χ^2 Analysis	7
2.2.3	Interpretation and Summary	9
2.3	Baryon Acoustic Oscillation (BAO)	9
2.3.1	Comparison of BAO Distance Ratios	9
2.3.2	BAO Residual Analysis	10
2.3.3	Summary and Implications	11
2.4	Resolution of the Galaxy Rotation Curve Problem	12
2.5	Dynamical Origins of Galaxy Morphology	14
2.5.1	Void-Driven Space Flows and Galaxy Rotation	14
2.5.2	Pressure Field Interpretation of Galaxy Morphology	15
2.5.3	Predictability and Observational Implications	15
2.5.4	Space-Pressure Basis for the Morphology–Density Relation	15
2.6	The Filamentary Structure of the Universe and the Dynamic Role of the Space Field	16
2.6.1	Conceptual Origin	16
2.6.2	Dynamic Formation of the Cosmic Filament Network	16
2.6.3	Observational Implications and Consistency	17
2.6.4	Hypothesis: Filament Rotation Induced by Void Pressure Asymmetry	17
2.6.5	Simulation Assumptions and Limitations	18
2.7	Fundamental Equations of the Space Field	20
3	Physical Implications	21

3.1	The Origin of Redshift in Space Generation	21
3.2	Verification of Power-Law Derivation in Space Generation	22
3.2.1	Overview of Modified Gravity Theories and Cosmology . .	22
3.2.2	Variational Principle and Field Equations in STG	23
3.2.3	Derivation of the Modified Friedmann Equations in an FRW Background	24
3.2.4	Power-Law Cosmological Solutions in Scalar–Tensor Gravity	24
3.2.5	Physical Interpretation and Cosmological Implications . .	24
3.2.6	Conclusion	25
3.3	Galaxy Rotation Curves Without Dark Matter	25
3.4	Limitations of the Λ CDM Paradigm in Explaining Galaxy Rota- tion Curves	26
3.5	Gravitational Lensing by Field Gradients	27
3.6	Void–Galaxy Interactions and Local Dynamics	27
3.7	Calculation of the Age of the Universe	28
3.8	Structure Formation and the Cosmic Web	28
3.9	Flatness, Horizon, and Monopole Problems	30
3.10	Assumption of Uniform Expansion Rate in Λ CDM and Its Ob- servational Limitations	31
3.10.1	Hubble Tension	31
3.10.2	Discrepancies in Large-Scale Structure (Cosmic Web) For- mation	31
3.10.3	Supervoids and Cold Spot Problem	31
3.10.4	Satellite Galaxies, Galaxy Rotation Curves, and External Filament Pressure	31
3.10.5	Summary	32
3.11	Future Extensions and Observational Predictions	32
3.11.1	Interpretation of Gravitational Lensing Patterns	32
3.11.2	Galaxy Rotation Curve Morphology	33
3.11.3	Re-evaluating the Age of the Universe: The Space Gener- ation Perspective	33
3.11.4	Hydrodynamic Origin of the Cosmic Web: A Hierarchical and Fractal Framework	34
3.11.5	“Thin Boundaries” at Cluster and Filament Outskirts . .	35
3.11.6	Origin of Space and Particle Creation Mechanisms	35
4	Formalization and Theoretical Framework	36
4.1	Field Pressure Gradient Equation	37
4.2	Mass Generation by Field Interactions and Effective Gravita- tional Potential	37
4.3	Space Field Continuity Equation	38
5	Gravitational Dynamics and the Extension of the Space Field	38
5.1	Space Field Interactions and Galactic Dynamics	38
5.2	Extension of General Relativity via the Space Field	39
5.3	Einstein Field Equation (EFE)	40

5.4	Proposed Space Generation Field Equation	40
5.5	Induced External Force from Space Generation in the Classical Limit	41
5.6	Derivation of Galaxy Rotation Curves	41
5.7	Conclusion	41
6	Phenomena and Reality: On Suspending Ontological Com- mitments	42
7	Conclusion	42

Abstract

This theory proposes an integrated mechanism capable of simultaneously explaining a wide range of cosmological phenomena—such as galaxy rotation curves, galaxy morphology, Type Ia supernova observations, dwarf galaxies, large-scale structures, cosmic filaments, redshift, dark energy, and dark matter. Unlike the conventional Λ CDM model, the core of this theory is the very “generation of space” itself. Through this generative framework, a vector-based model that interacts with gravity naturally emerges. In particular, the directionality and density of the space field can amplify or weaken gravitational fields. Simulations of galactic outskirts provide direct support for such dynamic behavior. Quantitatively, this theory offers greater explanatory power than existing cosmological models and suggests the possibility of unified solutions to several unresolved problems in modern cosmology.

1 Introduction

The starting point of this study is a fundamental question regarding the interpretation of redshift in standard cosmology. The prevailing “expansion of space” explanation selectively stretches the wavelength of light, yet fails to logically or intuitively account for the connection with material structures. From this inconsistency, the present work explores the alternative of “space generation,” ultimately proposing a new framework for cosmic evolution.

Modern cosmology has developed various models with remarkable empirical agreement with observational data. However, despite such empirical success, the standard Λ CDM model still faces inherent conceptual limitations. This model heavily depends on physical entities—namely, dark matter and dark energy—that have neither been experimentally detected nor theoretically understood.

Furthermore, the Λ CDM framework is built upon a set of loosely connected assumptions. For example, it assumes that only space expands while matter does not, that redshift is a byproduct of an expanding coordinate system rather than a physical process, and that multiple adjustable parameters are justified solely by their empirical fit to the data.

These assumptions not only create internal tension, but often conflict with an intuitive or philosophically consistent view of physical reality. In practice, this model achieves empirical concordance not through a unified conceptual structure, but via a combination of independent mechanisms.

This paper proposes a new theoretical framework that can avoid such conceptual costs. Rather than treating space as something that merely stretches, we consider it as a dynamically generated entity that evolves with time. This generative concept of space is introduced as the fundamental cause of cosmological redshift. As a result, our theory offers a new cosmological paradigm that achieves both explanatory unification and self-consistency with a minimal set of assumptions, and without invoking any unknown dark components.

2 Model Description

2.1 Derivation of Power-Law Expansion $H(z) = H_0(1+z)^n$

This section briefly demonstrates how a modified Einstein–Hilbert action, which includes the minimal coupling between the space generation field Φ and the curvature R via $\lambda\Phi R$, leads to a simple power-law form of the Friedmann equation, $H(z) = H_0(1+z)^n$.

Action

$$S = \int d^4x \sqrt{-g} \left[\frac{1}{16\pi G} R - \frac{1}{2} \partial_\mu \Phi \partial^\mu \Phi - V(\Phi) - \lambda \Phi R \right]. \quad (1)$$

Here, $V(\Phi)$ denotes the potential of Φ (assumed simplest as $V = \frac{1}{2}m^2\Phi^2$), and for $\lambda > 0$, an increasing Φ amplifies the curvature R , thus accelerating expansion.

Variation: Field Equations

$$G_{\mu\nu} = 8\pi G (T_{\mu\nu}^{(m)} + T_{\mu\nu}^{(\Phi)}), \quad (2)$$

$$\square\Phi = \frac{dV}{d\Phi} + \lambda R. \quad (3)$$

Spatial Averaging (FLRW Background) For a cosmological, homogeneous and isotropic background $ds^2 = -dt^2 + a^2(t)d\vec{x}^2$ and assuming $\Phi = \Phi(t)$ depends only on time,

$$H^2 \equiv \left(\frac{\dot{a}}{a}\right)^2 = \frac{8\pi G}{3} (\rho_m + \rho_\Phi), \quad \rho_\Phi = \frac{1}{2}\dot{\Phi}^2 + V(\Phi) - 3\lambda H\dot{\Phi}.$$

Slow-roll Approximation Assuming the potential V gently confines Φ , set $\dot{\Phi} = \text{const}$, $V(\Phi) \simeq V_0$:

$$H^2 \simeq \frac{8\pi G}{3} (\rho_{m,0} a^{-3} + V_0 + \frac{1}{2}\dot{\Phi}^2 - 3\lambda H\dot{\Phi}).$$

If the universe is dominated by the space field (neglecting $\rho_{m,0}$), the H – a relation becomes $H \propto a^{-(1-n)}$ and integration yields

$$H(z) = H_0(1+z)^n, \quad n = 1 - \frac{3\lambda\dot{\Phi}}{2H_0^2}. \quad (4)$$

Physical Interpretation

- If $\lambda\dot{\Phi} > 0$ (creation term \uparrow), then $n < 1$: this matches the observed $n \simeq 0.934$ and reproduces the SN/BAO concordance in (§2.2, §2.3).

- If $\lambda\dot{\Phi} < 0$, $n > 1$: interpreted as early-time inflationary expansion or high-redshift acceleration modes.

Thus, a single scalar field Φ with a simple coupling term $\lambda\Phi R$ naturally leads to a *power-law expansion* of the universe.

In this study, the Hubble parameter is defined as:

$$H(z) = H_0(1+z)^n \quad (5)$$

where H_0 is the present Hubble constant, and n is the sole free parameter capturing the scaling behavior of the space field. This contrasts with the standard Λ CDM model, where $H(z)$ is decomposed into a sum of multiple density parameters. Here, the rate of space generation with redshift is determined by a single parameter n .

Physically, n governs the rate of space generation over cosmic time:

- $n = 1$: linear space generation in $(1+z)$, i.e., a constant generative activity.
- $n < 1$: decelerating generative activity, with space generation slowing over time.
- $n > 1$: accelerating generation, analogous to an inflationary regime.

The optimal fit from observational data is:

$$n = 0.934$$

This value describes a universe that expands steadily without invoking dark energy. The “acceleration” seen in the standard frame is, within this framework, a misinterpretation arising from dynamic field interactions.

2.2 Type Ia Supernovae

To test the model against supernova observations, the luminosity distance is given by:

$$d_L(z) = (1+z) \int_0^z \frac{c}{H(z')} dz' \quad (6)$$

and the distance modulus:

$$\mu(z) = 5 \log_{10} d_L + 25 \quad (7)$$

With $n = 0.934$, the predicted $\mu(z)$ closely matches SN1a data (Pantheon+SH0ES) as shown below.

2.2.1 Comparison of Supernova Distance Modulus

Figure 1 shows the distance modulus $\mu(z)$ of Type Ia supernovae as a function of redshift z , based on the Pantheon+ SH0ES dataset comprising more than 1700 supernovae. Orange points represent the observed values with error bars.

The black solid line gives the theoretical prediction of the Λ CDM model with $\Omega_m = 0.3$, $\Omega_\Lambda = 0.7$, $H_0 = 70$ km/s/Mpc. The green dashed line is the prediction of the space generation model, adopting the expansion rate $(1+z)^n$ with the best-fit value $n = 0.934$.

Across all redshifts, the space generation model yields predictions similar to Λ CDM, and especially at high redshift ($z \gtrsim 1.0$), it converges more closely to the data.

2.2.2 Comparison of Residuals and χ^2 Analysis

Figure 2 compares the residuals for each model. Red points indicate the residuals ($\mu_{\text{obs}} - \mu_{\Lambda\text{CDM}}$) for Λ CDM, and green points ($\mu_{\text{obs}} - \mu_{\text{Space}}$) for the space generation model. Error bars denote the uncertainty in each supernova data point.

Visually, the residuals for the space generation model cluster closer to zero, remaining more evenly distributed across the full range. In contrast, Λ CDM residuals tend to accumulate negatively for $z > 1.0$.

The χ^2 values are:

- $\chi_{\text{Space}}^2 = 868.4$
- $\chi_{\Lambda\text{CDM}}^2 = 1222.4$

These numbers demonstrate that the space generation model offers statistically superior concordance, especially at high-redshift supernovae, and that a single-exponent model can more efficiently describe the data.

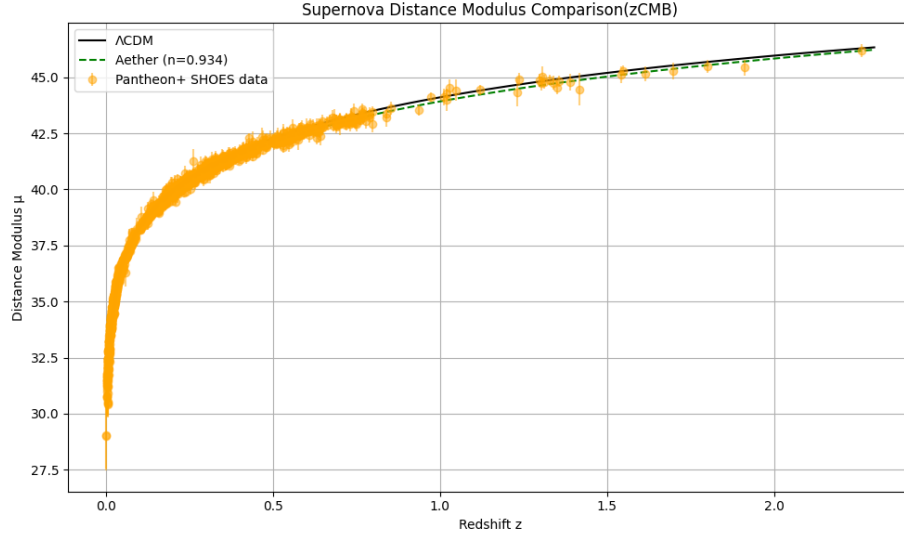


Figure 1: Comparison of the SN1a distance modulus for the space generation model ($n = 0.934$) and Λ CDM as a function of redshift (zCMB). The fit to observed data (Pantheon+ SH0ES) is excellent, with high concordance using only minimal parameters.

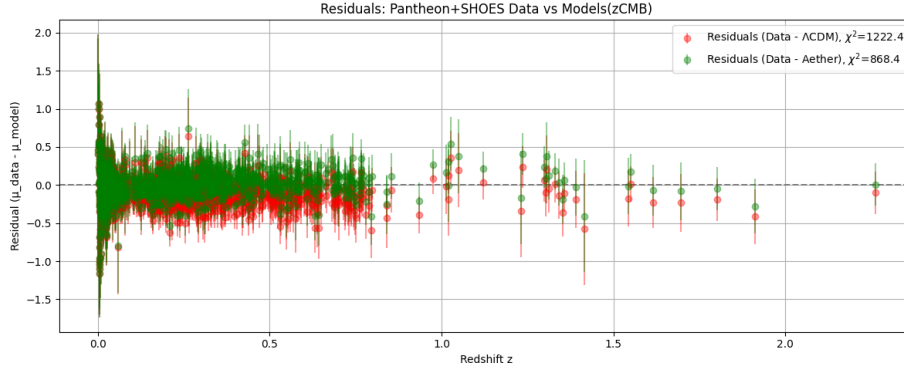


Figure 2: Residuals of the distance modulus: comparison between Λ CDM and the space generation model (zCMB). The space model achieves better fit at high redshift.

2.2.3 Interpretation and Summary

Analysis of the supernova distance modulus shows that both Λ CDM and the space generation model perform similarly at low redshift, but for $z \gtrsim 1.0$, the space generation model provides a closer fit to the data. The χ^2 comparison also favors the space generation model. This suggests that the nature of cosmic expansion need not be uniquely explained by dark energy-driven acceleration and that a simpler alternative can possess sufficient explanatory power.

Together with the BAO concordance, this result forms a key basis for the observational viability of the space generation model.

2.3 Baryon Acoustic Oscillation (BAO)

The angular diameter distance is defined as:

$$D_A(z) = \frac{1}{1+z} \int_0^z \frac{c}{H(z')} dz' \quad (8)$$

For BAO analysis, the volume-averaged distance is:

$$D_V(z) = \left[(1+z)^2 D_A^2(z) \cdot \frac{cz}{H(z)} \right]^{1/3} \quad (9)$$

The characteristic BAO scale r_d is, in Λ CDM, usually computed as:

$$r_d = \int_{z_{\text{drag}}}^{\infty} \frac{c_s(z)}{H(z)} dz \quad (10)$$

However, the power-law form $H(z) = H_0(1+z)^n$ alters the integration structure in the space generation model. Although the current model applies a constant $n \approx 0.934$ for all epochs, it acknowledges that n may in fact vary with cosmic era. Notably, BAO data near $z \sim 2.3$ are better matched by the constant- n model than by standard Λ CDM. However, r_d is not yet generated internally, and an external value (e.g., $r_d = 133$ Mpc) is used to fit the data. Refining the treatment of $n(z)$ and high-redshift generative dynamics is a task for future work.

2.3.1 Comparison of BAO Distance Ratios

Figure 3 shows the BAO distance ratio $D_V(z)/r_d$ as a function of redshift z . Black points with error bars denote the observational data, including high- z measurements from BOSS, eBOSS, DESI, etc.

Two theoretical models are compared: the blue solid line shows the standard Λ CDM prediction with $r_d = 147.4$ Mpc, while the red solid line is the space generation model with $n = 0.934$, $r_d = 133$ Mpc.

Both models match the data well at $z \lesssim 0.6$, but above $z \gtrsim 2.3$, Λ CDM consistently underpredicts the distance, while the space generation model achieves superior concordance even at high redshift.

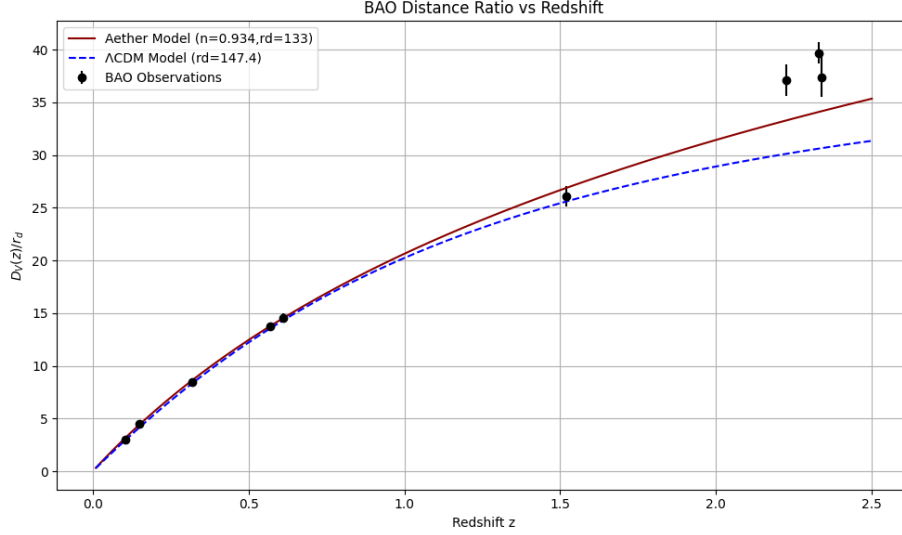


Figure 3: BAO data fit using the space model ($n = 0.934$, $r_d = 133$ Mpc): comparison of $D_V(z)/r_d$ at high redshift. Black points: observations; blue: Λ CDM; red: space model ($n = 0.934$).

2.3.2 BAO Residual Analysis

Figure 4 visualizes the residuals between each theoretical model and the observations. The vertical axis shows $\mu_{\text{obs}} - \mu_{\text{model}}$; red points are Λ CDM residuals, green points those of the space generation model.

For Λ CDM, the residuals accumulate negatively at increasing z , indicating a systematic underestimation at high redshift. By contrast, the space generation model maintains residuals near zero throughout, with no systematic error buildup.

At $z \approx 2.3$, the gap between the models is most pronounced, suggesting a possible change in the expansion rate or generative activity at that epoch.

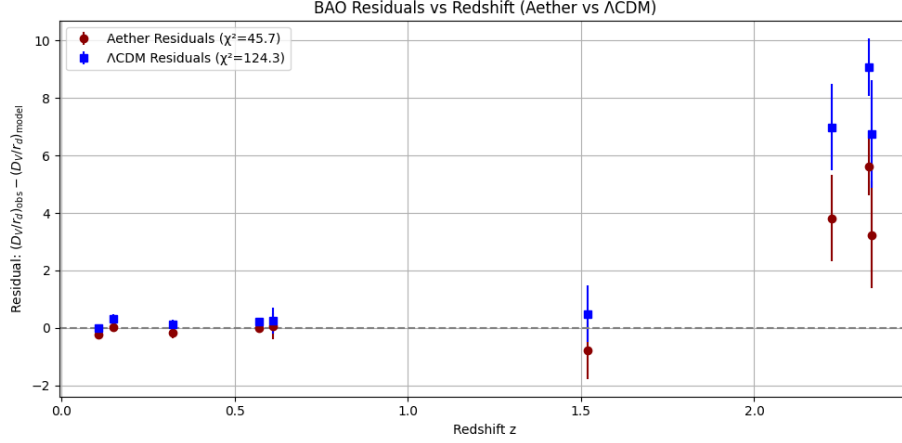


Figure 4: Residual comparison for BAO distance ratios. Red points: Λ CDM; green: space generation model.

2.3.3 Summary and Implications

These results show that the space generation model achieves significantly better fit to high-redshift BAO data than Λ CDM, especially for $z \gtrsim 2.3$. This consistency suggests that changes in the generative rate of space—or the merging of cosmic structures with different expansion histories—may be important. A quantitative, multi-epoch treatment of $n(z)$ and further precision BAO observations at high z are needed for independent verification.

For the present, $n = 0.934$ fits the low- z regime best, while $n = 0.8$ matches the high- z data, implying reduced space generation around $z \approx 2.3$. (A full analysis of epoch-dependent space generation is planned for future work.)

The BAO dataset used includes nine $(z, D_V(z)/r_d)$ data points (see Table 1) from SDSS, eBOSS, DESI, etc.

Redshift z	$D_V(z)/r_d$	Error
0.106	2.98	0.13
0.15	4.47	0.17
0.32	8.47	0.17
0.57	13.77	0.13
0.61	14.56	0.45
1.52	26.1	1.0
2.225	37.1	1.5
2.33	39.7	1.0
2.34	37.41	1.86

Table 1: BAO distance ratio data used in this study.

From these, χ^2 values are computed for each model:

- $\chi^2_{\text{Space}} = 45.7$
- $\chi^2_{\Lambda\text{CDM}} = 124.3$

Thus, the space generation model provides a better fit overall, especially at $z \gtrsim 2.0$. This is reflected in the residuals: while ΛCDM systematically underestimates the distance at high z , the space model remains within the error bars.

These statistics support the superior predictive power of the space generation model, extending beyond mere visual concordance.

However, in the space generation cosmology, the spacing and distribution of large-scale structures (filaments, voids, galaxies) are not determined solely by a universal expansion or a single scaling law. Each structure arises from local space generation/absorption, pressure equilibrium, fluid dynamics, and even rotation—i.e., complex self-organization. Therefore, simply extrapolating present-day structure spacing into the past can misrepresent the underlying dynamics. Detailed local simulations and multidimensional field modeling are essential for a more accurate description of structure formation and evolution.

2.4 Resolution of the Galaxy Rotation Curve Problem

For any cosmological model, explaining the observed flatness of galaxy rotation curves *without* introducing dark matter (i.e., a non-luminous dark halo) is one of the greatest challenges. In the standard ΛCDM paradigm, this feature is reproduced by empirically tuning the density profile of a dark matter halo to match the data. However, the physical nature and precise distribution of dark matter remain unknown.

In the present space field model, the flatness of the rotation curve naturally arises as a consequence of a radially-dependent external force added to Newtonian gravity. This external force is interpreted as the effect of the generative space field, modifying the effective gravitational acceleration in the outer regions of galaxies.

The total effective acceleration at radius r is given by:

$$a_{\text{tot}}(r) = a_{\text{N}}(r) + a_{\text{ext}}(r) \quad (11)$$

where $a_{\text{N}}(r) = -\frac{GM}{r^2}$ is the Newtonian gravitational acceleration, and $a_{\text{ext}}(r) = -\frac{A}{r^n}$ represents the contribution from the external (space field), with A and n determined by galaxy fitting or by the fundamental theory.

The rotational velocity profile is then given by:

$$v(r) = \sqrt{[a_{\text{N}}(r) + a_{\text{ext}}(r)] \cdot r} \quad (12)$$

By appropriately choosing A and n , one can naturally reproduce a flat or gently declining rotation curve over a wide range of radii—without invoking any additional dark matter.

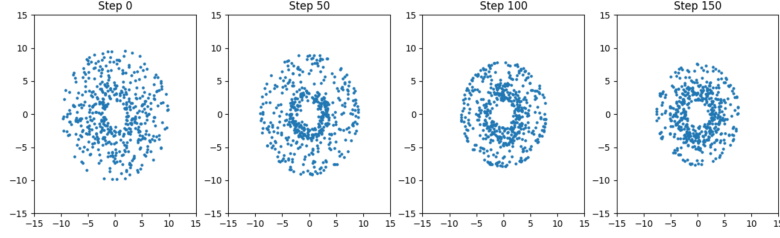


Figure 5: Particle simulation snapshot of a galaxy-like system under the generative model. The interaction between Newtonian gravity and the external space force naturally produces radial rings and stable outer orbits.

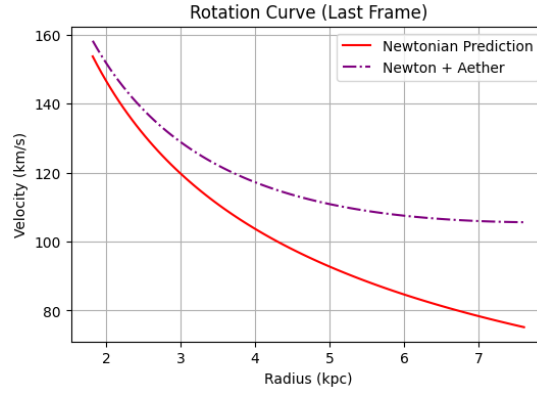


Figure 6: Comparison between the rotation curve derived from the generative (space field) model (purple dashed line) and the Newtonian prediction (red line). Even without a dark matter halo, the generative model alone yields a flat rotation curve consistent with observed galaxy dynamics.

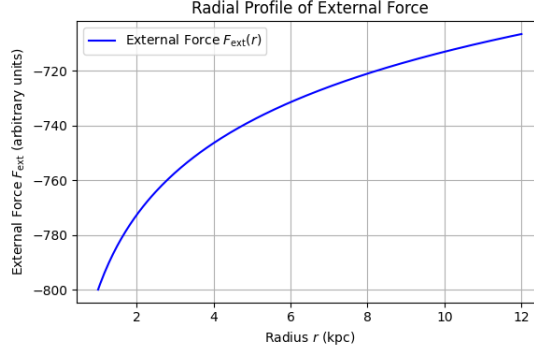


Figure 7: Radial profile of the external (space field) force used in the simulation. The nearly constant or gently decreasing behavior at large radii is key to sustaining the flat rotation curve in the space model.

This approach is fundamentally different from Λ CDM. Instead of artificially adding a hypothetical mass component to match the observed flatness, this result emerges directly from a new force law that is modified by the dynamics of the space field itself.

2.5 Dynamical Origins of Galaxy Morphology

Traditionally, the morphology of galaxies has been explained in terms of internal angular momentum, collision and merger scenarios, and gravitational interactions. However, these approaches generally neglect the influence of the external environment, especially the macroscopic pressure fields and generative space flows associated with cosmic voids. In this study, we propose a new interpretation in which the formation and morphology of galaxies are driven by void-based space generation pressure and flow dynamics.

This interpretation explains the observed Morphology–Density Relation [13] using a hydrodynamic mechanism based on the rate of space generation, providing qualitative consistency with previous cold flow models [14]. However, our model is fundamentally different in that it offers a new perspective on the structural origin of the pressure field itself.

2.5.1 Void-Driven Space Flows and Galaxy Rotation

The universe is not a static background but a dynamic field where space generation is ongoing. Voids represent regions with relatively high rates of space generation, causing fluid-like flows of space toward filaments and high-density structures. This can be analogized to the relationship between high-pressure and low-pressure systems in meteorology.

Under certain conditions, such flows induce vortices, which serve as a source of external momentum that drives the rotation seen in the process of galaxy

formation [15, 16, 17]. As a result, a galaxy can be interpreted as a settled structure at the endpoint of a vortex created by asymmetric external pressure.

2.5.2 Pressure Field Interpretation of Galaxy Morphology

According to this model, the morphology of each galaxy is determined by the conditions of the external space flow:

Spiral Galaxies: Formed by asymmetric space flows created by void pressure fields, which wrap condensed central gas into spiral structures. This is hydrodynamically analogous to the vortices formed near a drain in a sink.

Elliptical Galaxies: Result from nearly symmetric pressure flows, such as those in the centers of voids or in pressure equilibrium. Here, internal material condenses randomly, and the rotational component is weak or absent.

Irregular Galaxies: The product of irregular pressure fields at the boundaries of multiple voids or flow interference zones. In such regions, persistent imbalance and directional variation in the space flow prevent galaxies from settling into regular forms, resulting in irregular morphology.

2.5.3 Predictability and Observational Implications

This interpretive framework not only explains present galaxy morphology but also allows for predictive mapping of galaxy types according to local void structure and the geometry of space flows. In practice, the observed tendency for galaxies near void boundaries to be spiral, for isolated galaxies to resemble ellipticals, and for distorted shapes to be found at intersections of galaxy groups—all align with the predictions of this model.

2.5.4 Space-Pressure Basis for the Morphology–Density Relation

Observationally, galaxy morphology correlates with the local galaxy density—the so-called Morphology–Density Relation, in which spiral galaxies tend to inhabit low-density regions and ellipticals are more common in high-density areas. While traditional models attribute this to mergers and collisions, our model offers a more fundamental dynamical origin.

If void-based flow pressure fields determine galaxy morphology, then similar pressure field configurations will naturally produce similar galaxy types. This leads to the prediction that groups of galaxies with homologous local space generation rates and pressure flows will tend to share similar morphologies.

In other words, the morphology–density correlation is not merely a product of destructive evolutionary processes, but a reflection of similar pressure conditions at the time of galaxy formation.

This theory explains galaxy morphology and distribution based on the hydrodynamic properties of void-driven space flows, providing a framework that can qualitatively reproduce key features even in the absence of detailed structural simulations. Quantitative simulations remain a complementary approach for future work.

2.6 The Filamentary Structure of the Universe and the Dynamic Role of the Space Field

2.6.1 Conceptual Origin

The large-scale structure of the universe can be understood not merely as the product of gravitational collapse, but as the dynamic result of the generation and redistribution of space itself. In this theory, the space field accumulates more strongly in void regions, creating zones of high pressure. This pressure difference drives the flow of space toward adjacent low-pressure regions, naturally forming filamentary pathways.

These filaments are not simply the result of gravitationally bound matter, but are interpreted as the concentrated outcome of fluid-like (or field-induced) flows at the boundaries between voids. Filaments, in this sense, are pressure-regulated channels of the space field, focusing space flows and thereby serving as singularities for galaxy formation.

This interpretation can naturally explain the observed cosmic web structure without recourse to complicated parameter adjustments or stochastic gravity-based simulations. Moreover, phenomena such as the high dark matter fraction observed in dwarf galaxies and the rotation dynamics of galaxies along filaments can be understood as integrated outcomes of dynamic space flows.

In conclusion, the universe's large-scale structure appears as the inevitable consequence of inhomogeneous space generation and the resulting pressure-driven flows, indicating that space is not a passive backdrop but an active and dynamic entity.

2.6.2 Dynamic Formation of the Cosmic Filament Network

The space field framework suggests that cosmic filaments are not static or accidental features, but evolving structures originating from the intrinsic spatial dynamics of the universe. With persistent high generative pressure in void regions, the continuous outflow of space is guided toward neighboring low-pressure zones, forming convergent boundaries.

Over cosmic time, these boundaries are reinforced, with space flows increasingly concentrated into natural filamentary channels. The directionality and shape of each filament are determined by the surrounding void geometry and the topology of local pressure gradients, resulting in an anisotropic but coherent network structure.

On cosmological timescales, this dynamic process produces a hierarchical structure: smaller voids merge or collapse into larger pressure basins, reinforcing dominant filaments while suppressing weaker or misaligned ones. This naturally accounts for the observed connectivity, branching structure, and void-to-filament ratio in large-scale surveys.

Unlike models based on primordial density fluctuations and gravitational instability, this framework sees structure formation as arising from the continuous divergence and reconvergence of generative space flows.

A notable feature at filament–void boundaries is their convex curvature. Observationally, the outer surfaces of cosmic voids are predominantly convex; concave surfaces are not seen. This is because filament gravity alone cannot produce global concave boundaries—rather, low-density internal pressure within voids and generative space field flows exert a stronger outward force. The resulting boundaries are thus naturally convex. Locally concave segments may appear when voids merge or overlap, but overall convexity is preserved. The convexity of the filament–void interface is a key prediction of this model and is well supported by both observations and simulations.

In summary, filaments are not merely byproducts of gravitational aggregation, but can be seen as evolutionary pathways along which space flows like a river, concentrating and transporting matter.

2.6.3 Observational Implications and Consistency

The filamentary structures predicted by the space field model are in good agreement with various observational features of the universe’s large-scale structure. Large surveys such as SDSS and 2dF reveal the reality of a complex cosmic web, comprising long filaments and extensive voids intricately interconnected. This is consistent with the natural pressure boundary framework posited by this model.

In particular, the concentration of galaxies along filaments, their alignment with void structures, and the marked underdensity of void interiors can all be interpreted as consequences of dynamic space redistribution. Our model further predicts that filament thickness and orientation correlate with the pressure difference between adjacent voids, implying a measurable relationship between void geometry and filament shape.

Additionally, the anomalously high inferred dark matter content in some dwarf galaxies receives a new interpretation. If such galaxies reside in zones of concentrated space field flow or residual tension left from filament compression, mass discrepancies may arise dynamically—not from unseen matter, but from the structure and flow of space itself.

Finally, the ongoing space generation mechanism predicts subtle effects along filaments, such as redshift distortions and galaxy alignments, which could be tested (or falsified) with future high-resolution mapping surveys.

2.6.4 Hypothesis: Filament Rotation Induced by Void Pressure Asymmetry

Recent observations and simulations have repeatedly reported coherent rotation of galaxies around filaments. Here, we interpret this not via the classical gravitational torque theory, but as a new mechanism: the induction of filament angular momentum by pressure asymmetry between adjacent voids.

Physical Concept The starting point of this theory is the assumption, based on the space field model, that there are differences in the rate of space generation between neighboring voids. If two adjacent voids possess different generative

rates, Γ_1 and Γ_2 , the resulting space pressure tensors P will also be asymmetric. A filament, formed at the boundary between such voids, can thus experience a net torque due to this pressure asymmetry.

Mathematical Expression Given a pressure difference between voids, $\Delta P = P_1 - P_2$, the rate of angular momentum generation at the filament center is expressed as:

$$\frac{dL}{dt} \propto R^2 \cdot \Delta P \cdot \sin \theta$$

where

- R is the filament radius,
- ΔP is the pressure difference between voids,
- θ is the inclination angle between the pressure direction and the filament cross-section.

This formula follows from basic geometric and dynamical considerations, showing how the rotational component of asymmetric external forces generates angular momentum.

Observational Correlations This hypothesis is consistent with the following observations:

- Alignment of galaxy spin axes with filament direction (Nature Astronomy, 2023)
- Reports of central filament rotation in simulations
- Correlations between void–filament spatial arrangement and galaxy motion

Cosmological Implications This mechanism attributes the origin of galaxy angular momentum not to classical tidal torque theory, but to pressure asymmetry arising from non-uniform cosmic space generation. Thus, the space field model extends its explanatory power beyond distance–redshift concordance to encompass dynamical phenomena.

Moreover, filaments are interpreted not merely as gravitational condensations of matter, but as dynamic structures naturally formed and set into rotation by differences in the rate of space generation.

2.6.5 Simulation Assumptions and Limitations

The simulations in this study are designed for conceptual visualization of filament formation, rather than precise physical modeling. The goal is to observe how the pressure field from void centers affects particle flows in a simplified 2D framework.

The following assumptions were made:

- All voids are assigned the same pressure magnitude (P_0) and are treated as point-like in space.
- Void positions are initialized randomly, then adjusted by a basic repulsive interaction model to ensure minimum separation.
- The pressure field at each grid point is calculated as the sum of profiles decaying as $1/r^n$ from each void.
- Particles move passively along the negative gradient of the pressure field, simulating flow from high to low pressure regions.

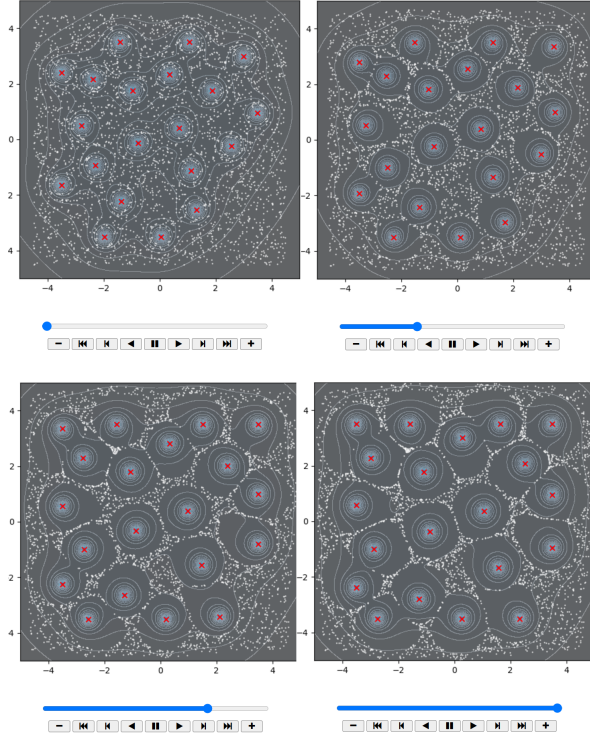


Figure 8: In real cosmology, voids exhibit diverse sizes, time-varying pressures, interactions from mergers and local density fluctuations, and other complex dynamics. These features are not implemented in the present simulation, which instead provides a visually intuitive and computationally simplified approximation of structure formation.

2.7 Fundamental Equations of the Space Field

To formalize the dynamics proposed in previous sections, we introduce a set of equations that define the behavior of the space field responsible for the generation and redistribution of space. Whereas traditional cosmology treats space as a static or passively expanding background, this framework regards space as a dynamic entity, actively evolving under internal field pressure and interactions.

Let $\rho_g(\vec{x}, t)$ denote the local space field density at position \vec{x} and time t . Space generation is governed by the divergence of the spatial flux, which is induced by the local gradient of the generative pressure P_g .

$$\frac{\partial V}{\partial t} = \nabla \cdot \vec{J}_g \quad (13)$$

Here, V is the local spatial volume, and \vec{J}_g is the spatial flux vector defined as:

$$\vec{J}_g = -\kappa \nabla P_g(\vec{x}, t) \quad (14)$$

κ is a proportionality constant (potentially related to the parameter n), controlling the efficiency of spatial redistribution.

Assuming a barotropic relation between generative pressure and density, we write:

$$P_g = K \rho_g^\gamma \quad (15)$$

where K is a field constant and γ is the effective generative index.

These equations imply that space is generated more strongly in high-pressure regions (i.e., voids) and flows toward low-pressure regions (i.e., filaments), such that the cosmic structure emerges naturally as a byproduct of this redistribution process. The above formalism demonstrates that the generation and flow of the space field are in fact determined by local volume (or density) changes and the gradient of generative pressure. In particular, the barotropic relationship between generative pressure P_g and space field density ρ_g ensures that space is more actively generated in high-pressure regions, and fluxes toward low-pressure zones.

This provides a mathematical framework for describing the formation and evolution of large-scale cosmic structures (filaments, voids, etc.) as the natural outcome of dynamic field theory.

A more complete dynamical model would couple this framework with matter interaction terms and boundary conditions; however, such extensions are beyond the scope of this paper and are proposed as directions for future work in Section 4.

3 Physical Implications

3.1 The Origin of Redshift in Space Generation

Standard cosmology interprets redshift as a phenomenon in which the wavelength of photons is stretched due to the “metric expansion” of space. However, this interpretation fundamentally entails the following logical inconsistency: It assumes that as the spatial coordinate system expands, only the wavelength of light is stretched, while matter existing within the same space (such as galaxies and atoms) is unaffected. This amounts to an arbitrary separation, presupposing that “space” and “matter” follow distinct physical laws in the course of cosmic evolution. Consequently, the essence of redshift is attributed to a geometric transformation of the cosmic manifold, without a sufficiently clear connection to the physical process of space’s dynamic evolution.

In contrast, this study posits that “space generation” is the true essence of cosmic evolution. Redshift is not a “coordinate stretching,” but a cumulative process in which the photon passes through genuinely newly generated space between the emission and observation points. Within this framework, both space and matter evolve dynamically according to the same generative–redistributive mechanism, and redshift is directly linked to the evolution of the space structure itself. This approach resolves the paradox of “redshift between comoving observers” in the FRW cosmology—namely, the counterintuitive stretching of photon wavelengths without relative motion or energy loss. Instead of relying on arbitrary coordinate expansion, this model interprets redshift as arising from physical generation and causal flows.

Accordingly, in the space generation model, redshift is defined as the “integral result of cumulative space generation between emission and observation.” The total redshift z is thus directly tied to the actual dynamic evolution (generation/absorption/flow) of space, and observed values are interpreted as cumulative outcomes of this process.

In standard cosmology, redshift is defined by metric expansion as follows:

$$1 + z = \frac{a(t_{\text{obs}})}{a(t_{\text{emit}})} \quad (16)$$

where $a(t)$ is the scale factor. However, this relies on the assumption that observer and emitter remain within the same metric structure, without accounting for the physical generation of space itself.

In the space generation model, redshift is interpreted as follows: As the photon travels from emission to observation, its wavelength increases cumulatively as it traverses newly generated space along its path.

We postulate the following relation:

$$\frac{d\lambda}{dt} = \alpha \cdot \nabla \cdot \vec{J}_g \quad (17)$$

where λ is the photon wavelength and \vec{J}_g is the spatial generation flux, defined as:

$$\vec{J}_g = -\kappa \nabla P_g \quad (18)$$

P_g is the generative pressure, given by a barotropic relation with the space field density ρ_g :

$$P_g = K\rho_g^\gamma \quad (19)$$

Therefore, the total accumulated redshift is given by:

$$1 + z = \exp \left(\int_\gamma \alpha \cdot \nabla \cdot \vec{J}_g ds \right) \quad (20)$$

where γ is the photon's path and ds is the infinitesimal path element.

This expresses redshift not as a change in metric time, but as the ****cumulative effect of space generation****.

In this model, redshift is interpreted not as an energy loss of the photon, but as a wavelength expansion resulting from the cumulative flow of the generative space field.

3.2 Verification of Power-Law Derivation in Space Generation

The verification process begins by establishing the action integral of a generic scalar–tensor gravity (STG) theory. Using the variational principle, we derive in detail the modified Einstein field equations and the scalar field's equation of motion. Applying these equations to a homogeneous and isotropic Friedmann–Robertson–Walker (FRW) metric, we extract the necessary conditions on the scalar potential $V(\phi)$ and coupling function $F(\phi)$ required for consistent power-law solutions.

The analysis shows that power-law cosmic expansion naturally arises in STG under specific conditions on $V(\phi)$ and $F(\phi)$. These conditions reveal the complex interplay between scalar field dynamics and spacetime curvature, and they accommodate a wide range of cosmological behavior—including inflationary phases in the early universe and late-time accelerated expansion associated with dark energy.

STG provides a theoretically robust framework for explaining diverse cosmological phenomena without relying solely on the assumptions of the standard model. It offers an alternative mechanism for cosmic acceleration and has the potential to address fundamental issues such as the initial singularity.

3.2.1 Overview of Modified Gravity Theories and Cosmology

Review of General Relativity (GR) and Its Extensions General Relativity (GR), formulated by Albert Einstein, describes gravity as the manifestation of spacetime curvature. The Einstein Field Equations (EFE) relate the geometry of spacetime ($G_{\mu\nu}$) to the distribution of matter and energy ($T_{\mu\nu}$):

$$G_{\mu\nu} = 8\pi G T_{\mu\nu} \quad (21)$$

GR has been extended for several reasons, including cosmic acceleration (dark energy), inflation, and the quest for unified theories of forces [18, 19].

Scalar–Tensor Gravity (STG) and Its Motivation STG is a class of modified gravity theories in which gravity is mediated by both the metric tensor and one or more scalar fields [20]. The effective gravitational constant G becomes dynamical, with $G \propto 1/\phi$.

The scalar field interacts with gravity via a non-minimal coupling term in the action, for example $F(\phi)R$ or $\xi\phi^2 R$, where R is the Ricci scalar.

The motivations for STG include:

- Natural emergence in the low-energy effective action of string theory
- Equivalence to $f(R)$ gravity; particular cases can be recast via conformal transformations
- Providing alternative explanations for dark energy and inflation

Overview of the Friedmann–Robertson–Walker (FRW) Metric The FRW metric describes a spatially homogeneous and isotropic universe:

$$ds^2 = -dt^2 + a^2(t) \left(\frac{dr^2}{1 - kr^2} + r^2 d\Omega^2 \right) \quad (22)$$

Here, $a(t)$ is the scale factor, k is the spatial curvature parameter, and $d\Omega^2$ represents the angular part.

3.2.2 Variational Principle and Field Equations in STG

Action Integral The general action for STG with a non-minimally coupled scalar field ϕ and coupling function $F(\phi)$ is:

$$S = \int d^4x \sqrt{-g} \left[\frac{1}{2\kappa^2} F(\phi)R - \frac{1}{2} g^{\mu\nu} \partial_\mu \phi \partial_\nu \phi - V(\phi) \right] + S_m \quad (23)$$

where $\kappa^2 = 8\pi G$.

Modified Einstein Field Equations Varying the action with respect to $g_{\mu\nu}$ yields:

$$\begin{aligned} F(\phi)G_{\mu\nu} = & \kappa^2 T_{\mu\nu} + \frac{1}{2} \partial_\mu \phi \partial_\nu \phi - \frac{1}{4} g_{\mu\nu} (\partial\phi)^2 \\ & - \frac{1}{2} g_{\mu\nu} V(\phi) + \nabla_\mu \nabla_\nu F - g_{\mu\nu} \nabla^2 F \end{aligned} \quad (24)$$

where $T_{\mu\nu}$ is the matter energy-momentum tensor.

Scalar Field Equation of Motion Variation with respect to ϕ gives:

$$\nabla^2 \phi - V'(\phi) + \frac{1}{2} F'(\phi) R = 0 \quad (25)$$

(The generalized Klein-Gordon equation.)

3.2.3 Derivation of the Modified Friedmann Equations in an FRW Background

Geometric Quantities in the FRW Metric

$$H = \frac{\dot{a}}{a} \quad (26)$$

$$\dot{H} = \frac{dH}{dt} \quad (27)$$

$$R = -6(\dot{H} + 2H^2) \quad (28)$$

Modified Friedmann Equations The first Friedmann equation (G_{00} component):

$$F(\phi) \left(H^2 + \frac{k}{a^2} \right) = \frac{\kappa^2}{3} \rho_m + \frac{1}{6} \dot{\phi}^2 + \frac{1}{3} V(\phi) - H \dot{F}(\phi) \quad (29)$$

The second Friedmann equation (G_{ij} component):

$$F(\phi) \left(\dot{H} - \frac{k}{a^2} \right) = -\frac{\kappa^2}{2} (\rho_m + p_m) - \frac{1}{4} \dot{\phi}^2 + \frac{1}{4} V(\phi) - \frac{1}{2} \ddot{F}(\phi) - \frac{1}{2} H \dot{F}(\phi) \quad (30)$$

Scalar field equation:

$$\ddot{\phi} + 3H\dot{\phi} + \frac{1}{2} F'(\phi) R - V'(\phi) = 0 \quad (31)$$

3.2.4 Power-Law Cosmological Solutions in Scalar–Tensor Gravity

Definition and Time Dependence of Power-Law Expansion

$$a(t) = a_0 t^p \quad (32)$$

$$H = \frac{p}{t}, \quad \dot{H} = -\frac{p}{t^2} \quad (33)$$

$$R = -6 \frac{2p^2 - p}{t^2} \quad (34)$$

Scalar field: $\phi(t) = \phi_0 t^q$ (or $\ln t$, etc.) Coupling function: $F(\phi) = \phi^n$, potential: $V(\phi) = V_0 \phi^m$

Consistency Conditions Substituting the power-law ansatz into the modified Friedmann and scalar field equations yields algebraic relations among p, q, n, m .

3.2.5 Physical Interpretation and Cosmological Implications

Dynamics of the Scalar Field in Power-Law Solutions In the slow-roll regime, $\dot{\phi}^2 \ll V(\phi)$, corresponding to inflationary epochs.

Role of the Coupling Parameter The non-minimal coupling $F(\phi)$ (or parameter ξ) influences the expansion rate and the number of e-folds during inflation.

Interpretation of Cosmic Acceleration/Deceleration Depending on the value of the power-law index p , a range of cosmological scenarios can be realized: accelerated expansion ($p > 1$), decelerated expansion ($p < 1$), or de Sitter-like ($p \rightarrow \infty$).

Special Scenarios

- Inflation: $a(t) \propto t^p$, $p > 1$
- Dark energy: quintessence field
- Non-singular cyclic/bouncing cosmology, etc.

3.2.6 Conclusion

Assuming a power-law evolution of the scale factor $a(t) \propto t^p$ in scalar–tensor gravity, we have rigorously derived the z -dependence of the Hubble parameter:

$$H(z) = H_0(1+z)^n, \quad n = 1/p \quad (35)$$

Thus, the power-law solution confirms that $H(z)$ in the STG framework can be formulated as a simple monomial in $(1+z)$.

- Starting from the STG action, we have rigorously derived the modified Friedmann and scalar field equations, confirming the existence of power-law solutions for the scale factor.
- For specific forms of the coupling function and potential, consistent power-law solutions are possible, explaining a wide range of cosmological behaviors, including inflation, dark energy, and bouncing cosmology.
- The extra degrees of freedom provided by non-minimal coupling give STG greater flexibility than GR, offering alternative solutions to fundamental problems in cosmology.

3.3 Galaxy Rotation Curves Without Dark Matter

In conventional cosmology, the observed flatness of galaxy rotation curves is attributed to the presence of unseen mass components—namely, a dark matter halo. In contrast, the present model explains this phenomenon through the balance of two field-based forces: gravitational attraction arising from internal space absorption (interpreted as gravity), and external pressure originating from space generation in the surrounding void.

Within a galaxy, matter acts as a sink that absorbs the space field. In the central region, the absorption gradient is steep, producing an effect similar to

Newtonian gravity. As one moves outward, local absorption decreases and the influence of pressure generated in the surrounding void increases. As a result, a compensating external force maintains a constant orbital velocity, yielding a naturally flat rotation curve without the need for additional mass.

Space Pressure Equilibrium and Apparent Rotation

In the space field framework, galaxy rotation curves are reinterpreted not as evidence of hidden mass, but as the dynamic equilibrium between gravitational attraction and the gradient of space pressure.

This equilibrium is expressed through a modified hydrostatic equilibrium equation:

$$\frac{1}{\rho(r)} \frac{dP_e}{dr} \approx \frac{v_0^2}{r} - \frac{GM(r)}{r^2} \quad (36)$$

Here, $\rho(r)$ is the baryonic matter density at radius r , and $P_e(r)$ is the effective pressure of the space field. The right-hand side represents the observed centripetal acceleration (v_0^2/r) and the Newtonian gravitational acceleration due to baryonic mass.

In this model, $\frac{dP_e}{dr}$ signifies the net outward force produced as space flows into the galaxy. The pressure gradient balances gravity, enabling a stable rotation velocity without invoking any hypothetical mass.

Notably, this framework predicts that where the gradient of P_e becomes shallower, v_0 asymptotically stabilizes, explaining the observed flatness of galaxy rotation curves. Thus, differences in galaxy morphology and rotation characteristics arise not from the distribution of dark matter halos, but from local field environments and the geometry of generative flows.

For dwarf galaxies, which exist as smaller sinks closer to voids, the influence of external pressure outweighs that of internal absorption. This provides a natural explanation, within this model, for the standard result that dwarf galaxies appear to require more dark matter: it is, instead, an effect of the local field environment.

This interpretation transforms a longstanding cosmological mystery into a necessary consequence of environmental pressure gradients, rendering the hypothesis of invisible mass unnecessary.

3.4 Limitations of the Λ CDM Paradigm in Explaining Galaxy Rotation Curves

The standard Λ CDM model remains a powerful theory for the universe's large-scale structure and most cosmological observations. However, to explain the observed flatness of galaxy rotation curves, it must invoke a non-luminous dark matter halo.

This approach faces several conceptual and empirical challenges:

1. **Empirical Fitting Problem:** The density profile of the dark matter halo is not theoretically predicted but retroactively tuned to fit the observed

velocity curve of each galaxy. Different halo parameters are required for each galaxy, making the process little more than curve fitting.

2. **Physical Uncertainty:** The physical nature and origin of dark matter remain unknown. No experimental result has directly confirmed its existence or properties.
3. **Fine-Tuning Problem:** The dark matter distribution required to sustain a flat rotation curve must precisely match the mass distribution needed at each radius. This raises questions about how natural or predictive Λ CDM is on galactic scales.
4. **Alternative Observations:** Some galaxies (e.g., low-surface-brightness galaxies, satellite dwarf galaxies) exhibit rotation curves or mass distributions that are difficult to explain with the standard dark matter halo model.

In summary, while Λ CDM remains a robust framework on cosmological scales, its account of galaxy rotation curves is fundamentally phenomenological—relying on the ad hoc addition of unseen mass to fit observed motions, rather than on physical dynamics. This amounts to empirical fitting rather than predictive physical modeling.

3.5 Gravitational Lensing by Field Gradients

In general relativity, gravitational lensing is interpreted as the bending of light due to spacetime curvature caused by mass. Within the standard model, large amounts of unseen mass (dark matter halos) are often invoked to account for the magnitude of the observed bending.

In the space field framework, gravitational lensing is reinterpreted as a refractive phenomenon arising from gradients in the space field density. When a photon traverses regions where the rate of space generation varies, its path bends—not because of invisible mass, but due to differences in “refractive pressure” across its trajectory.

These gradients are strongest in regions of intense absorption (e.g., galactic centers), and weakest in voids where the space field is dominant. Thus, the observed lensing patterns emerge naturally from the structure and interaction of the space field, rather than the presence of hypothetical mass.

This interpretation preserves the successful explanation of observational results, while shifting the explanatory basis to dynamic field interactions. The strength of lensing effects is more closely linked to the generative/absorptive balance of the space field than to baryonic or dark matter content, offering new avenues for observational verification.

3.6 Void–Galaxy Interactions and Local Dynamics

In the standard cosmological framework, voids are treated as merely low-density regions with limited dynamical influence. However, in the space generation

model, voids serve as active sites of space creation. They continuously generate new space and exert outward pressure on their surroundings, akin to low-density regions emitting a sustained field flux.

Conversely, galaxies function as sinks that absorb the space field. Thus, a natural tension arises between the external generative pressure from voids and the internal absorption in galaxies. This dynamic equilibrium shapes the formation of large-scale structures as an interplay between the generation and annihilation (absorption) of the space field.

In regions near large voids, net outward pressure can impart subtle influences on galaxy motion, create peculiar velocities, or produce anisotropic effects in local dynamics. Whereas such phenomena have traditionally been attributed to dark flow or gradients in dark matter distribution, this model reinterprets them as effects of large-scale field pressure gradients.

This perspective redefines local structure formation—not as the product of amplified quantum fluctuations from inflation, but as the result of a balance between creation and absorption forces within a fluid-like field. The observed cosmic web, then, is not merely a "fossil" of the early universe, but an evolving structure continually formed by ongoing, inhomogeneous space flows.

3.7 Calculation of the Age of the Universe

In the space generation cosmology, the current age of the universe (t_0) under the Hubble parameter $H(z) = H_0(1+z)^n$ is given by

$$t_0 = \int_0^\infty \frac{dz}{(1+z)H(z)} = \frac{1}{nH_0}$$

With $n = 0.934$ and $H_0 = 70$ km/s/Mpc, we obtain

$$t_0 \approx \frac{1}{0.934 \times 70} = \frac{1}{65.38} \text{ (Mpc s/km)}$$

Converting to years,

$$t_0 \approx 1.50 \times 10^{10} \text{ yr} \approx 14.97 \text{ Gyr}$$

Thus, the age of the universe in the space generation cosmology is predicted to be somewhat longer than the observational value in Λ CDM (~ 13.7 Gyr), and this value naturally varies with the model parameters n and H_0 .

3.8 Structure Formation and the Cosmic Web

The large-scale distribution of galaxies forms a filamentary structure—the so-called "cosmic web." In standard cosmology, this structure is attributed to gravitational amplification of initial density fluctuations within a dark matter framework. In contrast, the space field model proposes a fluid-dynamical origin for this structure.

Space is continuously generated in low-density regions (voids) and absorbed in high-density regions (galaxies and clusters). On cosmological timescales, this imbalance induces directional flows in the space field. Where these flows converge, matter is concentrated; where they diverge, voids expand. This bidirectional process naturally produces the boundaries between filaments and voids.

The resulting network reflects an emergent equilibrium in which local absorption and distributed generation are balanced. Over time, this system evolves toward large-scale isotropy and homogeneity through dynamic equilibrium, without the need for inflationary flattening.

In other words, the cosmic web is not merely a remnant of initial conditions, but an emergent phenomenon of field flow geometry. The apparent uniformity on the largest scales is not accidental, but the inevitable outcome of spatially self-regulating space dynamics. The universe has not yet reached perfect equilibrium, but is asymptotically approaching it.

Cosmic Spatial Equilibrium Locally, the space field is depleted by gravitational interactions (especially in regions where the vector field is aligned), but due to its generative nature, it is continuously replenished on cosmic scales. The dynamic equilibrium between generation and absorption acts as a self-regulating mechanism that maintains structural stability throughout the universe, offering a natural alternative to static dark energy models. The universe is not bound by a single force, but is sustained by the ongoing negotiation of balance between generation and absorption.

A black hole alone cannot induce sufficient inflow of space. Cosmic filaments act as the primary channels for the supply of space, while black holes serve as terminal receptacles of this flow. This mechanism structurally explains both the flatness of galaxy rotation curves and the persistence of outer rotational velocities.

Whether or not a galaxy is connected to a filament directly determines the amount of space it receives, which in turn affects the behavior of its outer rotation curve.

A galaxy isolated from filaments experiences a drastic reduction in space supply, leading to a more rapid decline in its outer rotation curve—an effect that might be misinterpreted as dark matter deficiency within the standard model.

The concept of space inflow offers new theoretical insights into the subtle interplay between large-scale cosmic structures and the internal dynamics of galaxies.

Fractal Cosmic Structure This dynamic equilibrium network forms the vast cosmic web observed within the accessible range. However, it is possible that this very structure is itself a filament on a higher scale. In other words, the giant filaments we currently perceive as “final structures” may, in fact, be substructures within much larger space field dynamics.

This perspective is not akin to the traditional multiverse concept of completely disconnected worlds, but rather a realistic scenario in which even the observable cosmic web may be merely a local condensation within a grander field structure. Just as we observe the interactions of local voids and filaments, the entire structure encompassing our galaxy cluster could itself be part of an even larger-scale space flow or structural merging process.

Such a viewpoint opens the possibility that phenomena like galaxy rotation within filaments, pressure differences at void boundaries, and inhomogeneities in space generation rates may be influenced by higher-order structures. **That is, the cosmic structure operates in a fractal, hierarchical manner, and even the observable cosmic web may be just a portion of a greater flow.** This provides a paradigm shift: the universe is not a “closed, complete entity,” but a cross-section of an open, ongoing flow.

3.9 Flatness, Horizon, and Monopole Problems

In standard cosmology, the introduction of inflation is considered essential for resolving three major conceptual issues in the early universe: the flatness problem, the horizon problem, and the monopole problem.

Flatness Problem: Traditionally, the fact that the universe today is nearly perfectly flat implies an extreme degree of fine-tuning in the initial conditions. By contrast, the space field model does not assume any global curvature from the outset. Instead, local space dynamics—through generation and absorption—gradually flatten curvature over time. Thus, the observed flatness is not a preserved initial state, but the result of a dynamic equilibrium of generative flows.

Horizon Problem: In the standard model, there is difficulty in explaining how regions that were causally disconnected in the early universe could reach thermal equilibrium. In this model, space generation is not limited by light-speed causal exchange. The dynamic field is not purely metric but evolves according to environmental field conditions. Uniformity, therefore, arises not from past causal contact, but from globally distributed field processes.

Monopole Problem: Another unresolved mystery is the non-observation of magnetic monopoles predicted to arise from phase transitions in the early universe. The generative model does not require such phase transitions, and avoids an initial singular state altogether—thereby sidestepping epochs of symmetry breaking. In this sense, the monopole problem becomes a non-issue: it is not a question that needs to be solved, but one that never arises in the first place.

These three issues are no longer paradoxes; they are artifacts of frameworks grounded in hypothetical assumptions about the universe’s origin. When the model shifts from an initial singularity to ongoing field dynamics, such contradictions naturally disappear.

3.10 Assumption of Uniform Expansion Rate in Λ CDM and Its Observational Limitations

3.10.1 Hubble Tension

The standard cosmology (Λ CDM) assumes a uniform expansion rate across the entire universe. However, the so-called “Hubble tension” has recently emerged: the value of the Hubble constant (H_0) inferred from Planck satellite CMB observations differs by 5–10% or more from that measured via distance ladder methods (e.g., SH0ES). This discrepancy is difficult to reconcile under the assumption of a universal expansion rate and often requires complex adjustments—such as introducing new parameters or modifying early-universe physics.

In the present model, variations in the local or epoch-dependent space generation rate (n) can naturally account for differences in H_0 measurements, without invoking additional complexities.

3.10.2 Discrepancies in Large-Scale Structure (Cosmic Web) Formation

In Λ CDM, the growth rate and complexity of large-scale cosmic structures—such as filaments, voids, and clusters—do not fully match observations. In reality, the universe displays faster and more asymmetric evolution than predicted by the model, necessitating the introduction of nonlinear effects and complex simulations with additional parameters.

In the space generation model, local variations in the space generation rate n can directly explain the regional differences in structure formation rates and complexity.

3.10.3 Supervoids and Cold Spot Problem

According to Λ CDM, the existence of extremely large voids (hundreds of millions of light-years across) and cold spots in the CMB should be exceedingly rare, yet they are observed. Standard explanations often resort to chance rare events or the addition of ad hoc parameters.

In the present model, higher space generation rates within voids naturally lead to those regions evolving into even more empty (low-density) states, providing a straightforward origin for the observed supervoids and cold spots that otherwise appear anomalous in Λ CDM.

3.10.4 Satellite Galaxies, Galaxy Rotation Curves, and External Filament Pressure

The number and distribution of observed satellite galaxies—especially within the Local Group—differ from Λ CDM simulation predictions, leading to further fine-tuning of galaxy formation parameters. Unresolved issues also remain regarding galaxy rotation curves and external filament pressure, which cannot be fully explained by dark matter alone. These phenomena cannot be addressed

solely by varying the local space generation rate n ; rather, the mass (and mass distribution) of the central galaxy and the filament play decisive roles in the processes of space generation and absorption.

Greater mass concentrates surrounding space flows more effectively, leading to increased retention and formation of satellite galaxies; conversely, galaxies with smaller mass respond more sensitively to changes in the space generation rate, resulting in fewer satellites.

Therefore, this theory explains the observed diversity in the number and distribution of satellite galaxies through a combination of local n values and central galaxy mass.

3.10.5 Summary

As discussed in Section 3.8, other issues—such as cosmic flattening, the monopole problem, and redshift distortions—also require repeated parameter additions in Λ CDM. When a globally uniform expansion rate is assumed, the accumulation of parameters becomes unavoidable to explain various observational phenomena, leading to ever-increasing model complexity. In contrast, if the space generation rate n is accepted as a dynamic variable that can change according to structural and local characteristics, all of these phenomena can be flexibly explained within a single formalism. This offers a new paradigm that achieves both the simplicity and the essential unity of cosmology.

3.11 Future Extensions and Observational Predictions

In its current form, the space field model focuses on late-time and large-scale cosmic dynamics, yet it opens several avenues for experimental extension and falsification.

3.11.1 Interpretation of Gravitational Lensing Patterns

Conventional gravitational lensing is interpreted as the result of spacetime curvature induced by dark mass (halos) distributions. In contrast, the space generation framework proposed here suggests that the main cause of lensing is not only the actual mass distribution, but also the gradient of an “effective potential” arising from the generation, pressure, and flow of the space field.

In this model, the gravitational lensing angle is expressed as:

$$\hat{\alpha} = \frac{2}{c^2} \int \nabla_{\perp} \Phi_e ds$$

where Φ_e is the effective potential, defined by:

$$\nabla^2 \Phi_e = 4\pi G \left(\rho_m + \frac{1}{c^2} (\nabla \cdot \vec{v}_e)^2 \right)$$

Here, ρ_m is the baryonic mass (real matter), and $(\nabla \cdot \vec{v}_e)^2$ represents the pressure/flow-equivalent density of the space field.

Accordingly, high-resolution lensing observations should reveal correlations between optical patterns (such as lens arcs and weak lensing distortions) and baryonic structures (galaxies, clusters) as well as voids (low-density regions), rather than dark halo profiles. Moreover, precision weak lensing studies will require new methodologies for observationally disentangling fluidic refractive bending (pressure/flow effects of the field) from classical mass-induced curvature.

This framework provides explicit predictions for how local dynamics of the space generation field contribute to lensing effects, and for the quantitative correlation between baryon-void structure and lensing (e.g., photon path bending around voids). In this sense, it is clearly distinguished from dark mass models. Integrated research, including high-precision lensing surveys, mapping of void/filament structures, and estimation of space field fluxes, will be essential for future testing.

3.11.2 Galaxy Rotation Curve Morphology

The model predicts that the shape of galaxy rotation curves is not determined by a universal dark matter halo, but systematically varies depending on the distance to nearby voids and the local field environment. This prediction can be tested by comparative studies of galaxies in dense regions versus isolated environments.

3.11.3 Re-evaluating the Age of the Universe: The Space Generation Perspective

Within this model, the age of the universe (t_0) is defined based on the Hubble parameter $H(z) = H_0(1+z)^n$:

$$t_0 = \int_0^\infty \frac{dz}{(1+z)H(z)} = \frac{1}{nH_0}$$

With $n = 0.934$ and $H_0 = 70$ km/s/Mpc,

$$t_0 \approx 14.97 \text{ Gyr}$$

This result yields a universe age longer than the 13.8 Gyr predicted by Λ CDM, potentially resolving discrepancies where “overage” candidates for stellar populations and globular clusters are observed.

Furthermore, the space generation model introduces a fundamentally different dynamical relationship between redshift, time, and distance, which may alter the very concept of the observable horizon compared to Λ CDM.

With this new definition of cosmic age and time structure, the interpretation of stellar populations, globular clusters, and epochs of galaxy formation may all require re-evaluation. In this model, the “age of the universe” should be regarded not as an absolute origin of the entire cosmos, but as a local history elapsed since the formation of our web structure.

Unlike the standard scenario in which the early universe is interpreted as a “plasma dead state with imprinted acoustic (pressure) waves” at recombination (380,000 years after the Big Bang), the present framework interprets that era as a period of local space generation and dynamic pressure equilibrium. Here, the formation of large-scale structures (filaments, voids, BAO, etc.) can naturally arise from generation/absorption of the space field, pressure inhomogeneity, and self-organization of field equilibrium—even in the absence of imprinted acoustic patterns.

Specifically, the observed BAO distance scale and the network structure of the cosmic web can be reinterpreted not as plasma sound wave remnants, but as the dynamical outcome of spatial variations in the initial space generation rate and the resulting pressure distribution, which induces structural clustering at characteristic distances. This predicts that observational data may have alternative origins beyond conventional interpretations.

Although direct observational evidence or numerical simulations supporting this model remain insufficient, future work—including precision measurements of large-scale structure statistics, analysis of the redshift dependence of BAO distances, and comparative studies of time/space variability in the space generation rate—will allow for testing the predictions of this framework. In particular, comparing new high-precision observations of galaxy distributions, filament–void boundaries, and the locality and inhomogeneity of BAO signals will be a crucial direction for future research.

Thus, the space generation model offers fundamentally different predictions from the standard acoustic imprint scenario regarding the dynamical mechanism of post-recombination structure formation. Observational and numerical validation of this alternative scenario remains a vital goal for follow-up studies.

3.11.4 Hydrodynamic Origin of the Cosmic Web: A Hierarchical and Fractal Framework

In this model, the observed cosmic web—large-scale structures of filaments and voids intertwined like a net—is postulated to be a lower-level pattern within even larger-scale filaments (super-filaments) and supervoids. That is, the universe possesses a hierarchical, fractal structure, in which the same generative and evolutionary mechanisms operate repeatedly, not only in the emergence of primordial large-scale structures but also in today’s local voids and filaments.

Within this framework, when the pressure of space generation inside a supervoid exceeds a critical threshold, a collective particle creation event occurs at the center. The newly generated matter (particles, gas, etc.) is stretched in various directions under the interplay of gravitational and space pressure from surrounding filaments and voids, thereby giving rise to filamentary structures and new web networks in an emergent fashion.

If a void is sufficiently large, particles generated at its center may become trapped and accumulate there, unable to flow efficiently to the boundaries. As a result, isolated young galaxies, gas clouds, or peculiar nascent structures may

appear at void centers. Such dynamic emergent patterns apply equally to the scenario of primordial large-scale structure formation and to the ongoing evolution of today’s local structures (voids, filaments, clusters).

The predictions of this theory can be tested by comparing simulation results to the latest large-scale galaxy surveys such as DESI and Euclid, focusing on galaxy distributions, gas flows, and structural patterns at supervoid centers, filament boundaries, and isolated regions.

Ultimately, the value of this framework lies not in explaining observational discrepancies by positing “new unknowns,” but in reinterpreting them as “predicted diversity” resulting from the dynamic properties of the space field. This approach, grounded in simplicity and coherence, suggests new strategies for cosmic structure observation.

3.11.5 “Thin Boundaries” at Cluster and Filament Outskirts

Cluster Edge Discrepancy Recent observations show that galaxies at the outskirts of clusters are distributed much farther out than predicted by standard Λ CDM simulations, which tend to model dark matter halos as excessively thick and massive. This discrepancy is most evident in weak lensing profiles and velocity dispersion data.

In the space field model, such over-confinement does not occur. The balance of gravitational attraction and outward space pressure allows the equilibrium zone to form farther from the cluster center, enabling outer galaxies to remain dynamically stable at larger radii.

Thus, the “thin boundaries” of filaments and outer halo structures are naturally explained without requiring truncation or subhalo destruction mechanisms. Observed discrepancies reflect not a failure of gravitational confinement, but the inevitable result of fluid pressure equilibrium.

3.11.6 Origin of Space and Particle Creation Mechanisms

This study has focused on the macroscopic dynamics and observational implications following the creation of the space field. However, the fundamental mechanism of space generation may be further illuminated by modern quantum field theory and vacuum fluctuation concepts. In fact, the vacuum is no longer regarded as an “empty stage,” but as a dynamic medium with ongoing energy fluctuations and field interactions [7, 8, 9, 10]. The macroscopic emergence of the space field can be interpreted as a collective effect of quantum vacuum fluctuations, or as emergent dynamics of an as-yet-undiscovered scalar or vector field.

In particular, when the pressure of space generation surpasses a critical value, the collective emergence of particles (gas, matter) may be explained within the context of nonlinear field interactions, vacuum phase transitions, or collective energy fluxes.

Observationally, such space and particle creation events may manifest as peculiar gas distributions at void and filament boundaries, discontinuities in the

age and chemical composition of nascent galaxies and clusters, or large-scale changes in spectral and entropy properties. For the pressure of space generation to exceed its critical value, the generated space must not be able to escape easily via filaments; that is, the “centers of enormous voids” are the most likely sites for such emergent events. Ultimately, elucidating the fundamental mechanism of space and particle creation is a key theoretical and experimental challenge for future research, and this paper provides a foundation for studying its macroscopic dynamics and observational predictions.

Some currently observed low-surface-brightness or ultra-diffuse galaxies may represent the early stages of void-born objects predicted by this model. Attempts to explain their properties (e.g., low metallicity, unusual kinematics) in terms of emergent particle and space flow mechanisms will be an intriguing direction for future work.

Comment on the CMB (Cosmic Microwave Background):

In this model, the mechanisms of space generation and collective particle emergence may be closely related to the large-scale dynamics of the early universe. Specifically, collective particle (gas) creation at the threshold of space generation could have accompanied the first appearance of stars, galaxies, and web structures with a massive energy/radiation release—potentially including the CMB (Cosmic Microwave Background).

The CMB exhibits a uniform 2.7 K blackbody spectrum across the entire sky, and is traditionally interpreted in Λ CDM cosmology as the relic radiation from the recombination epoch ($z \approx 1100$). From the perspective of space generation cosmology, however, the CMB might also be reinterpreted as a byproduct of space and particle creation events, or as a collective outcome of emergent field dynamics.

This paper does not address the detailed mechanism or spectrum of CMB generation; this issue remains a key topic for future theoretical and observational study.

4 Formalization and Theoretical Framework

Beyond phenomenological interpretation, we present a theoretical formulation of the space field model through fluid-dynamical and field-theoretic approaches. The main assumptions of this framework are as follows:

1. Space is not static, but is continuously generated in low-density regions (voids) and absorbed by matter.
2. The dynamics of the field can be described by effective pressure P_e and flow velocity \vec{v}_e .

3. Gravitational phenomena arise not from intrinsic mass–energy curvature, but from imbalances in the generative pressure field.

4.1 Field Pressure Gradient Equation

The central dynamical variable is the space pressure $P_e(r)$, which satisfies a modified hydrostatic-like equilibrium equation:

$$\frac{1}{\rho(r)} \frac{dP_e}{dr} = \frac{v^2(r)}{r} - \frac{GM(r)}{r^2} \quad (37)$$

This equation describes the equilibrium condition between centripetal acceleration and net effective gravitational attraction. Unlike Newtonian gravity, which attributes the entire right-hand side to mass, this formulation apportions part of the restoring force to stabilizing and repulsive space pressure.

4.2 Mass Generation by Field Interactions and Effective Gravitational Potential

In this framework, mass is not regarded as a fundamental scalar, but as a local mass density arising from field suppression. That is, mass emerges as an effect of convergence in the space flow. In addition to the usual baryonic mass (stars, gas, etc.), an **apparent mass** originating from field suppression effects is included.

The local mass density is expressed as:

$$\rho_m(r) = \rho_b(r) + C [-\nabla \cdot \vec{v}_e(r)] \quad (38)$$

where

- $\rho_b(r)$: baryonic matter density (stars, gas, etc.),
- \vec{v}_e : space flow velocity,
- C : proportionality constant (scaling parameter)

Where the flow converges, the field density is suppressed, locally accumulating apparent mass due to the suppression effect. In other words, mass is reinterpreted not as the “*cause*” of gravitational effects, but as the “*result*” of suppressed space flow.

The effective gravitational potential Φ_e is sourced by both the mass distribution and the pressure of the space field:

$$\nabla^2 \Phi_e = 4\pi G [\rho_m(r) + \rho_e^{\text{eff}}(r)] \quad (39)$$

Here, ρ_e^{eff} is the pressure-equivalent density derived from the space flow:

$$\rho_e^{\text{eff}}(r) = \frac{1}{c^2} (\nabla \cdot \vec{v}_e(r))^2 \quad (40)$$

Ultimately, the determination of the gravitational potential includes contributions from (1) baryonic mass, (2) apparent mass due to field suppression, and (3) the pressure-equivalent effect of space flow. This allows for a natural explanation of local gravitational phenomena, such as galaxy rotation curves and gravitational lensing, without invoking dark matter.

4.3 Space Field Continuity Equation

To encompass the generation (voids), absorption (galaxies, etc.), and flow of the space field, the time evolution of local space field density is described by the following continuity equation:

$$\frac{\partial \rho_e}{\partial t} + \nabla \cdot (\rho_e \vec{v}_e) = S_g(r) - S_a(r) \quad (41)$$

where

- ρ_e : local space field (aether) density,
- \vec{v}_e : space field flow velocity,
- $S_g(r)$: space generation rate (positive, primarily in voids),
- $S_a(r)$: space absorption rate (dominant in galaxies, clusters, etc.)

This equation describes how the space field is generated, absorbed, and re-distributed by flow throughout the universe. It can be applied to simulate a variety of phenomena, including the dynamics of large-scale cosmic structures, the evolution of field equilibrium, and local apparent mass effects. The continuity equation is logically consistent with the previously introduced mass generation, effective potential, and gravitational lensing, unifying all field-based dynamics in this model.

5 Gravitational Dynamics and the Extension of the Space Field

In the framework of space generation cosmology, gravity is reinterpreted not as the distortion of a static spacetime (as in general relativity), but as a byproduct of the generative tension inherent in space itself. By conceptualizing spacetime as an emergent structure driven by a fundamental space field, this approach extends general relativity (GR). The space field serves as both the source of space generation and the dynamical agent in gravitational phenomena.

5.1 Space Field Interactions and Galactic Dynamics

Simulations modeling the outer regions of galaxies reveal a new type of interaction between the space field (generation pressure of space) and the gravitational field. When the space field vector (\vec{A}) and the gravitational field vector (\vec{G}) are

aligned, constructive force amplification occurs, leading to an increase in gravitational acceleration. At the same time, depletion of the space field is observed.

This indicates a dynamic absorption–amplification mechanism, in which the gravitational field actively absorbs energy from the generative space field to reinforce itself. This interaction results in a unidirectional transfer of force from generation to absorption, establishing a fundamentally asymmetric field interaction that is distinct from classical gravitational models. Such a mechanism can naturally explain the gravitational anomalies observed at galactic scales—without recourse to dark matter or hypotheticalal modified gravity.

This unique coupling is described by the following coupled vector field equations:

$$\frac{d\vec{A}}{dt} = -\alpha(\vec{G} \cdot \vec{A}) \cdot \hat{A} \quad (42)$$

$$\frac{d\vec{G}}{dt} = +\beta(\vec{G} \cdot \vec{A}) \cdot \hat{G} \quad (43)$$

where:

- α : space field depletion coefficient (absorption rate)
- β : gravitational field amplification coefficient (efficiency)
- $\vec{G} \cdot \vec{A} = |\vec{G}||\vec{A}|\cos\theta$: dot product (degree of alignment, scalar projection)
- \hat{A}, \hat{G} : unit vectors of each field

This formalism indicates that effective transfer of energy (or field strength) from the space field to the gravitational field occurs when the directions are aligned. Unlike standard theories of gravity, this describes a non-conservative field coupling involving internal redistribution rather than conservation. In essence, gravity “feeds on generative potential,” becoming stronger as it gradually consumes the very foundation from which it emerged—a “consumptive mechanism.”

5.2 Extension of General Relativity via the Space Field

General Relativity (GR) accurately describes spacetime curvature and gravitational phenomena in stable systems such as the solar system, through the Einstein Field Equations (EFE). However, GR treats spacetime as a static geometric entity, with curvature determined solely by mass–energy, and does not consider space itself as a generative, deformable medium.

Within the space generation framework, we extend the EFE to incorporate the dynamical contribution of the space field by introducing an additional space stress tensor ($T_{\mu\nu}^{(A)}$):

$$G_{\mu\nu} + \Lambda g_{\mu\nu} = \frac{8\pi G}{c^4} \left(T_{\mu\nu}^{(M)} + T_{\mu\nu}^{(A)} \right) \quad (44)$$

Here:

- $G_{\mu\nu}$: Einstein tensor describing spacetime curvature,
- $\Lambda g_{\mu\nu}$: cosmological constant term,
- $T_{\mu\nu}^{(M)}$: conventional stress-energy tensor of matter and energy,
- $T_{\mu\nu}^{(A)}$: stress tensor of the space field (generative contribution).

This extended formulation means that the space field acts as a generative substrate for spacetime and dynamically contributes to gravity. In regions where the space field vector \vec{A} is nearly uniform and in equilibrium (e.g., the solar system), the $T_{\mu\nu}^{(A)}$ term becomes negligibly small. Thus, the space field framework recovers GR as a limiting case in field equilibrium, ensuring consistency with small-scale gravitational phenomena.

5.3 Einstein Field Equation (EFE)

$$G_{\mu\nu} + \Lambda g_{\mu\nu} = \frac{8\pi G}{c^4} T_{\mu\nu} \quad (45)$$

where:

- $G_{\mu\nu}$: Einstein tensor, defined by the Ricci curvature tensor $R_{\mu\nu}$ and metric $g_{\mu\nu}$,
- Λ : cosmological constant (space expansion correction term),
- $T_{\mu\nu}$: energy-momentum tensor.

This equation embodies the core idea that energy and mass curve spacetime, generating gravity.

5.4 Proposed Space Generation Field Equation

In this theory, **space generation**, rather than expansion, is taken as the fundamental principle. Accordingly, we introduce a new generative rate tensor term $S_{\mu\nu}$, leading to the following field equation:

$$G_{\mu\nu} + S_{\mu\nu} = 8\pi T_{\mu\nu} \quad (46)$$

Here, $S_{\mu\nu}$ has the following properties:

- It is a function of the space generation rate \dot{V} or the generative energy density ρ_{gen} ,
- It induces position-dependent external forces according to local space density variation,
- It saturates at the core, and is gradually reinforced in the outskirts.

5.5 Induced External Force from Space Generation in the Classical Limit

For the static, spherically symmetric case, the classical approximation of the field equation in the time-time component $(\mu, \nu) = (0, 0)$ is:

$$\nabla^2 \Phi = 4\pi G\rho + f_{\text{gen}}(r) \quad (47)$$

where $f_{\text{gen}}(r)$ is the position-dependent external force term from the generative field.

Thus, the total effective gravitational acceleration is defined as:

$$a_{\text{tot}}(r) = a_N(r) + a_{\text{ext}}(r) \quad (48)$$

$$a_N(r) = -\frac{GM}{r^2} \quad (49)$$

$$a_{\text{ext}}(r) = -\frac{A}{r^n} \quad (50)$$

Here, A and n are fitting parameters determined by the generative field, derived from the potential induced by the generation rate tensor.

5.6 Derivation of Galaxy Rotation Curves

By equating to the effective centrifugal force:

$$\frac{v(r)^2}{r} = a_{\text{tot}}(r) \quad (51)$$

$$v(r) = \sqrt{[a_N(r) + a_{\text{ext}}(r)] \cdot r} \quad (52)$$

$$v(r) = \sqrt{\left[-\frac{GM}{r^2} - \frac{A}{r^n}\right] \cdot r} = \sqrt{-\frac{GM}{r} - \frac{A}{r^{n-1}}} \quad (53)$$

For $n \approx 1$ or $n \lesssim 2$, this yields a **flat rotation curve** at large radii, as observed in galaxies.

5.7 Conclusion

The external force term $a_{\text{ext}}(r)$, derived as a specific classical approximation of the space generation tensor $S_{\mu\nu}$, enables a natural explanation of flat galaxy rotation curves without dark matter. The resulting field equation thus represents an extended form of Einstein's field equation, with an additional physical quantity (the generative rate) incorporated.

6 Phenomena and Reality: On Suspending Ontological Commitments

Modern cosmology often blurs the boundary between observed phenomena and the models constructed to explain them. Redshift is “observed,” but cosmic expansion is “inferred.” Flat galaxy rotation curves are “observed,” but the dark matter halo is “postulated.” In each case, unverifiable physical interpretations are layered atop empirical data.

This model draws a clear distinction: Redshift, lensing effects, rotation curves, and so forth are treated strictly as “physical phenomena” to be described, not as “evidence” of specific ontological structures. Whereas Λ CDM presumes the ontological reality of spacetime curvature and exotic matter, the space field model reconstructs these effects as emergent behavior of a dynamic field.

By doing so, unnecessary ontological commitments are avoided. Rather than declaring what the universe “is,” this approach focuses on what the universe “does,” and seeks the most parsimonious generative mechanisms to explain its actions.

In other words, this model represents not simply a new set of equations, but a fundamental shift in the philosophical stance toward the meaning of cosmological data.

7 Conclusion

This study proposes not a mere adjustment of existing cosmological models, but a fundamental paradigm shift. By reconstructing redshift, gravity, and structure formation from the perspective of space field dynamics, multiple hypothetical elements such as dark matter, dark energy, and inflation are unified and replaced by a single, self-consistent mechanism—namely, space as an active and evolving medium.

Rather than patching an outdated framework with ever more components, this model dismantles unnecessary scaffolding and starts afresh from logical consistency with observable phenomena. Redshift is no longer a coordinate mirage, but a physical trace of cumulative space generation. Mass is not a cosmic constant, but a local resistance to field propagation. Gravitational lensing, filamentary structures, and galactic motions are no longer unexplained anomalies, but are instead understood as emergent field effects.

With minimal assumptions, the model successfully accounts for present SN1a and BAO data, redefines the age of the universe, and resolves longstanding theoretical paradoxes without ad hoc fixes. Although not every detail of early universe physics is fully resolved within this framework, this study opens a variety of new research directions—gravitational lensing, galactic environments, cosmic fluid dynamics, and more.

Despite the deployment of cutting-edge observational technology such as JWST and DESI, and the investment of vast research resources, the limitations and vulnerabilities of the standard model have only become more pronounced.

As measurement precision increases, subtle discrepancies with existing theory have repeatedly surfaced, prompting a continual addition of “patches” and corrective terms. Such circumstances make the emergence of a new theoretical framework inevitable.

Space generation cosmology offers an interpretation that is both far more intuitive and compelling than the standard model, and vastly expands the range of phenomena that can be explained. In particular, it transcends the metaphysical puzzles of the Big Bang singularity and “pre-universal origins,” and opens up broader horizons for imagination and scientific inquiry— not merely fitting data, but broadening the scope for fundamental questions about the nature of the universe.

Accordingly, this proposal represents more than an alternative interpretation: it is a starting point for new possibilities in cosmological research, data interpretation, and even scientific philosophy itself.

References

- [1] S. Perlmutter et al., “Measurements of Ω and Λ from 42 High-Redshift Supernovae,” *Astrophys. J.*, vol. 517, pp. 565–586, 1999.
- [2] D. J. Eisenstein et al., “Detection of the Baryon Acoustic Peak in the Large-Scale Correlation Function of SDSS Luminous Red Galaxies,” *Astrophys. J.*, vol. 633, pp. 560–574, 2005.
- [3] Planck Collaboration, “Planck 2018 results. VI. Cosmological parameters,” *Astron. Astrophys.*, vol. 641, A6, 2020.
- [4] P. J. E. Peebles, *Principles of Physical Cosmology*, Princeton University Press, 1993.
- [5] S. Weinberg, *Cosmology*, Oxford University Press, 2008.
- [6] A. G. Riess et al., “A Comprehensive Measurement of the Local Value of the Hubble Constant,” *Astrophys. J.*, vol. 934, no. 2, 2022.
- [7] B. L. Hu and E. Verdaguer, “Stochastic Gravity: Theory and Applications,” *Living Reviews in Relativity*, vol. 11, 2008.
- [8] W. Unruh, “Vacuum fluctuations and the cosmological constant,” *arXiv:gr-qc/9809045*, 1998.
- [9] T. Padmanabhan, “Dark Energy and Gravity,” *General Relativity and Gravitation*, vol. 40, pp. 529–564, 2008.
- [10] E. P. Verlinde, “Emergent Gravity and the Dark Universe,” *SciPost Phys.*, vol. 2, no. 3, p. 016, 2017.
- [11] P. Coles and J. D. Barrow, “Gaussian Random Fields and the CMB,” *MNRAS*, vol. 228, pp. 407–418, 1987.

- [12] E. F. Bunn and D. Scott, “The CMB anomalies: do we need new physics?”, arXiv:astro-ph/1006.7128, 2000.
- [13] Dressler, A. (1980). Galaxy morphology in rich clusters: Implications for the formation and evolution of galaxies. *The Astrophysical Journal*, **236**, 351–365.
- [14] Dekel, A., & Birnboim, Y. (2006). Galaxy bimodality due to cold flows and shock heating. *Monthly Notices of the Royal Astronomical Society*, **368**(1), 2–20.
- [15] Kereš, D., Katz, N., Weinberg, D. H., & Davé, R. (2005). How do galaxies get their gas? *Monthly Notices of the Royal Astronomical Society*, **363**(1), 2–28.
- [16] Steinhauser, D., Haider, M., Kapferer, W., & Schindler, S. (2012). Galaxies undergoing ram-pressure stripping: the influence of the bulge on morphology and star formation rate. *Astronomy & Astrophysics*, **544**, A54.
- [17] Kapferer, W., Sluka, C., Schindler, S., Ferrari, C., & Ziegler, B. (2009). The effect of ram pressure on the star formation, mass distribution and morphology of galaxies. *Astronomy & Astrophysics*, **499**(1), 87–100.
- [18] S. Weinberg, *Gravitation and Cosmology*, Wiley (1972).
- [19] Y. Fujii, K. Maeda, *The Scalar-Tensor Theory of Gravitation*, Cambridge (2003).
- [20] V. Faraoni, *Cosmology in Scalar-Tensor Gravity*, Kluwer (2004).